



Universiteit
Leiden

The Netherlands

Synthetic analogues of the histidine-chlorophyll complex: a NMR study to mimic structural features of the photosynthetic reaction center and the light-harvesting complex

Gammeren, A.J. van; Hulsbergen, F.B.; Erkelens, C.; Groot, H.J.M. de

Citation

Gammeren, A. J. van, Hulsbergen, F. B., Erkelens, C., & Groot, H. J. M. de. (2004). Synthetic analogues of the histidine-chlorophyll complex: a NMR study to mimic structural features of the photosynthetic reaction center and the light-harvesting complex. *Journal Of Biological Inorganic Chemistry*, 9(1), 109-117. doi:10.1007/s00775-003-0507-y

Version: Publisher's Version

License: [Licensed under Article 25fa Copyright Act/Law \(Amendment Taverne\)](#)

Downloaded from: <https://hdl.handle.net/1887/3464635>

Note: To cite this publication please use the final published version (if applicable).

Adriaan J. van Gammeren · Frans B. Hulsbergen
Cornelis Erkelens · Huub J. M. de Groot

Synthetic analogues of the histidine–chlorophyll complex: a NMR study to mimic structural features of the photosynthetic reaction center and the light-harvesting complex

Received: 17 July 2003 / Accepted: 29 October 2003 / Published online: 9 December 2003
© SBIC 2003

Abstract Mg(II)–porphyrin–ligand and (bacterio)chlorophyll–ligand coordination interactions have been studied by solution and solid-state MAS NMR spectroscopy. ^1H , ^{13}C and ^{15}N coordination shifts due to ring currents, electronic perturbations and structural effects are resolved for imidazole (Im) and 1-methylimidazole (1-MeIm) coordinated axially to Mg(II)-OEP and (B)Chl *a*. As a consequence of a single axial coordination of Im or 1-MeIm to the Mg(II) ion, 0.9–5.2 ppm ^1H , 0.2–5.5 ppm ^{13}C and 2.1–27.2 ppm ^{15}N coordination shifts were measured for selectively labeled [1,3- ^{15}N]-Im, [1,3- ^{15}N ,2- ^{13}C]-Im and [1,3- ^{15}N ,1,2- ^{13}C]-1-MeIm. The coordination shifts depend on the distance of the nuclei to the porphyrin plane and the perturbation of the electronic structure. The signal intensities in the ^1H NMR spectrum reveal a five-coordinated complex, and the isotropic chemical shift analysis shows a close analogy with the electronic structure of the BChl *a*–histidine in natural light harvesting 2 complexes. The line broadening of the ligand responses support the complementary IR data and provide evidence for a dynamic coordination bond in the complex.

Keywords (Bacterio)chlorophyll · Histidine · Imidazole · Magnesium porphyrin · 1-Methylimidazole

Abbreviations (B)Chl *a*: (bacterio)chlorophyll *a* · HMBC: heteronuclear multiple bond correlation · Im: imidazole · LH: light-harvesting · 1-MeIm: 1-methylimidazole · Mg(II)-Por: Mg(II)-porphyrin macrocycle · OEP: 2,3,7,8,12,13,17,18-octaethylporphyrin

Introduction

Chlorophyll (Chl) and bacteriochlorophyll (BChl) are the most abundant pigments of photosynthesis, which is the energetic basis of life on Earth. They are mainly found in the protein complexes of photosynthetic organisms, and are functional elements in light harvesting, energy transfer and electron transfer [1]. They are usually encapsulated in the light harvesting (LH) and photosynthetic reaction center complexes, which are the principal elements of the photosynthetic units of green plants and bacteria [2].

(B)Chl contains a Mg(II) ion in the center of the porphyrin macrocycle that is coordinated by four pyrrole nitrogens (Fig. 1). Two axial positions are available for the coordination of ligands to the Mg(II). From vibrational spectra and X-ray crystallographic analyses it was found that the Mg(II) of most (B)Chls in photosynthetic proteins are five-coordinated by the N $^{\delta}$ -atom from a histidyl residue in the protein. Owing to this coordination, the Mg(II) is slightly out of the equatorial plane [3, 4]. It has been reported that the Mg(II) out-of-plane distance of the five-coordinated [Mg(II)-OEP-pyridine] complex is 0.72–0.81 Å; since the Mg(II) ion of the five-coordinated structure is somewhat out of the plane, a second axial ligand coordination at the opposite side is thought to be less favorable [5]. Six-coordinated species are only formed in concentrated ligand solutions and in polar donor solvents that form solvate complexes and compete with the ligand for coordination to the Mg(II). It has been proposed that polarizable histidyl residues can be involved in stabilization of the charge separation process in photosynthesis [6]. This is supported by model studies that argued that charge–charge interactions between polar groups in the reaction center of *Rhodobacter sphaeroides* can give rise to a non-linear increase of the dielectric constant of the protein interior and stabilize a charged state [7].

A. J. van Gammeren · F. B. Hulsbergen · C. Erkelens
H. J. M. de Groot (✉)
Leiden Institute of Chemistry, Gorlaeus Laboratories, Leiden
University, P.O. Box 9502, 2300 RA Leiden, The Netherlands
E-mail: ssnmr@chem.leidenuniv.nl
Tel.: +31-71-5274539
Fax: +31-71-5274603

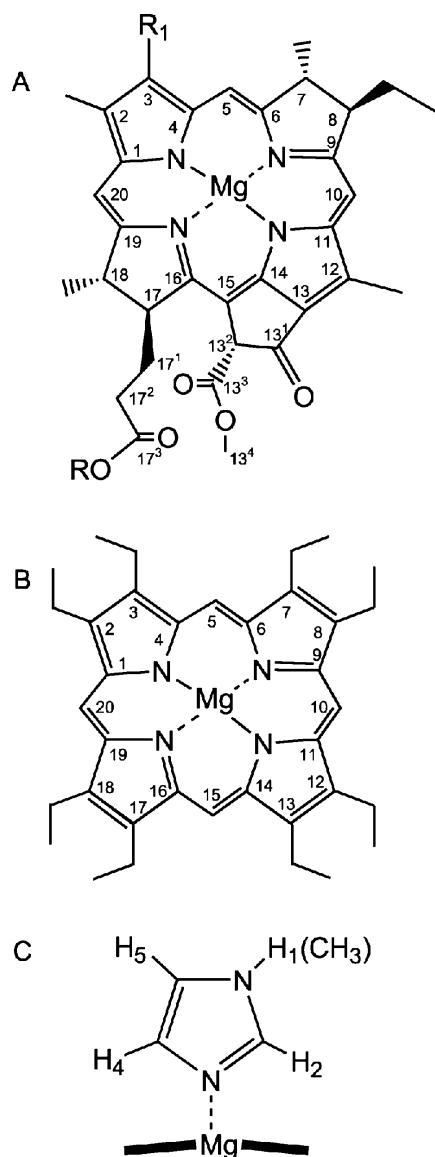


Fig. 1 **A** The structure of Bchl *a* ($R = \text{phytyl}$, $R_1 = \text{COCH}_3$) and Chl *a* ($R = \text{phytyl}$, $R_1 = \text{CH}=\text{CH}_2$). **B** The structure of Mg(II)-OEP. **C** A schematic figure of the axial coordination of a diazole ligand to the Mg(II)-porphyrin ring

A model study, in which NMR spectra were recorded on co-dissolved Im and (B)Chl *a* in THF, has proposed a negatively charged [(B)Chl *a*-Im] complex due to the deprotonation of the Im NH1 hydrogen [8]. The coordination behavior of imidazole and 1-methylimidazole (Im and 1-MeIm) to the Mg(II) of a series of Mg(II)-Por systems, including (B)Chl *a*, is here investigated by model studies in an attempt to mimic the neutral Mg(II)-histidyl coordination which is present in photosynthetic proteins. In a more general perspective, the information from these models is potentially also of interest for other metal-containing complexes like the heme proteins and vitamin B₁₂.

¹H and ¹³C NMR spectroscopy is used to monitor ¹H and ¹³C coordination shifts ($\Delta\delta$) for different

[ligand]:[Mg(II)-Por] molar ratios (r_m). The $\Delta\delta$ is the difference between the isotropic shifts of the free and the coordinated forms of the ligand and is due to the effect of the ring currents in the macrocycle of the porphyrin systems.

In addition to ¹H NMR spectroscopy, ¹⁵N NMR and ¹³C NMR can be applied to provide insight into the structure and electronic properties of the axially coordinated ligand. In particular, ¹⁵N NMR experiments are of interest, since the Mg(II) and the Im N-donor atom form a coordination bond, and the δ_N is very sensitive to the electronic configuration. In this work, ¹³C and ¹⁵N NMR experiments are performed using [1,3-¹⁵N,2-¹³C]-Im, [1,3-¹⁵N]-Im and [1,3-¹⁵N,1,2-¹³C]-1-MeIm. ¹⁵N labeling at both positions is relatively straightforward, while ¹³C nuclei can be incorporated conveniently at positions 1 and 2 [9].

The pyrrole-type (N1) and pyridine-type (N3) nitrogens, present in Im and 1-MeIm, each have very characteristic chemical shift ranges in ¹⁵N NMR spectra. The pyrrole-type signal is shifted by ~ 100 ppm from the resonance of the pyridine-type [10]. For Im in protic solvents or in concentrated solutions, the proton exchanges very rapidly in a tautomeric equilibrium, yielding an average chemical shift, $\bar{\delta}^{15}\text{N}$. In contrast, 1-MeIm shows two different ¹⁵N resonances, due to the presence of the methyl group. It has been reported that substitution of the hydrogen at the pyrrole-type nitrogen by a methyl group has only a marginal effect on the isotropic shift of the pyrrole-type nitrogen [11, 12].

Materials and methods

Synthesis

Labeled starting materials, all with 99% isotope incorporation, were purchased from Cambridge Isotopes Laboratories (Andover, Mass., USA) and used without further purification. For the synthesis of isotopically enriched Im and 1-MeIm, a known procedure was followed to obtain 1.08 g (15.4 mmol) of [1,3-¹⁵N,2-¹³C]-Im, 1.00 g (15.4 mmol) of [1,3-¹⁵N]-Im and 0.228 g (2.65 mmol) of [1,3-¹⁵N,1,2-¹³C]-1-MeIm [9]. The purity of Im obtained by two consecutive recrystallizations was $\sim 99\%$ and the material was used without further purification. To obtain a completely dry ligand solution for NMR investigations, 25 mg of ligand was dissolved in 5.0 mL CDCl₃ and dried over activated molecular sieves (3 Å) in a dry argon atmosphere.

An amount of 59.0 mg (0.11 mmol) of Mg(II)-OEP was prepared, starting from 100 mg (0.19 mmol) of metal-free OEP (Porphyrin Systems) and an excess of MgBr₂·OEt₂ (490 mg, 1.90 mmol) in CH₂Cl₂ [13]. The compound was washed with water. Subsequently, the Mg(II)-OEP was eluted rapidly from an alumina column (10×1.5 cm) with acetone (p.a. grade), giving 59.0 mg (0.11 mmol) of 97:3% Mg(II)-OEP/metal-free OEP.

The complex of Mg(II)-OEP with one axial Im or 1-MeIm ligand was achieved by dissolving Mg(II)-OEP with just sufficient warm isobutanol. To this solution a slight excess of ligand solution was added, and some drops of triethyl orthoformate were added for dehydration. After 1–2 days, the [Mg(II)-OEP-1,3-¹⁵N,1,2-¹³C-1-MeIm] complex appeared as small crystals in the solution. To obtain the crystalline [Mg(II)-OEP-1,3-¹⁵N-Im] complex, an amount of petroleum ether (100–120) equal to the isobutanol

volume was added to the complex solution and the mixture was placed for 14 days at $-35\text{ }^{\circ}\text{C}$. After crystallization the supernatant was decanted.

(B)Chl *a* isolation

A mixture of Chl *a* and Chl *b* was extracted from spinach leaves, using an efficient method described by Omata and Murata [14]. To separate Chl *a* from Chl *b*, a silica column (3.0×12 cm) was used. The fractions were slowly eluted with hexane/propanol (20:1). The first band that eluted from the column contained pure Chl *a*; the second band contained pure Chl *b*. The solvent of the Chl *a* solution was evaporated and the residue was stored under argon at $-35\text{ }^{\circ}\text{C}$ until it was used.

BChl *a* was isolated from a *Rhodobacter (Rb.) sphaeroides* R26 culture [15]. Briefly, bacteria were grown anaerobically in a sterile synthetic medium at $30\text{ }^{\circ}\text{C}$ and with a light intensity of 2700 lux. Each liter of medium contained: 0.75 g of algae hydrolysate, 1.00 g succinic acid, 2.6 mL 6.5 M NH_4OH , 20 mL of 1.0 M H_2KPO_4 , 20 mL of 1.0 M HK_2PO_4 , 0.60 g $\text{MgSO}_4\cdot 2\text{H}_2\text{O}$, 0.12 g NaCl, 0.050 g $\text{CaCl}_2\cdot 2\text{H}_2\text{O}$, 125 μL vitamin solution (1.0 g thiamine-HCl + 8.0 mg biotine in 20 mL 5% EtOH/ H_2O), 10 mg nicotinic acid, 10 mL of a trace element stock solution containing 316 mg/L FeCl_2 , 20 mg/L $\text{MnSO}_4\cdot \text{H}_2\text{O}$, 10 mg/L H_3BO_3 , 10 mg/L $\text{CuSO}_4\cdot 5\text{H}_2\text{O}$, 10 mg/L $\text{Na}_2\text{MoO}_4\cdot 2\text{H}_2\text{O}$, 20 mg/L ZnCl_2 , 200 mg/L $\text{CaCl}_2\cdot 2\text{H}_2\text{O}$ and 40 mg/L $\text{MgSO}_4\cdot 7\text{H}_2\text{O}$. The pH of the medium was adjusted with concentrated HCl to 6.8.

After growing for 8 days, the cells were harvested and the absorption of the cell culture was measured at 863 nm (A_{863} : 3.1 cm^{-1}). The cells were centrifuged (20 min at $15,000\times g$). The cell pellet was suspended in 20 mM Tris-HCl buffer (pH 8.5) and stored at $-35\text{ }^{\circ}\text{C}$. The cell pellet was thawed and a mixture of acetone/methanol (7:3) was added to extract the chromophores from the cells. The suspension was centrifuged to precipitate the cell fragments. The pigment-containing supernatant was concentrated and purified with a cross-linked agarose column (1.5×2.0 cm; Sepharose CL-6B). First a thin green band was eluted from the column, using hexane/acetone (20:1) as eluent. Subsequently, an intense blue band, containing the BChl *a*, was eluted easily from the column with pure acetone. The solution was concentrated and the pure BChl *a* was stored under argon at $-35\text{ }^{\circ}\text{C}$ until use.

Sample preparations

Activated molecular sieves (3 Å) were used to prepare anhydrous CDCl_3 . To exclude oxygen and moist from air, the sample preparation was performed under anaerobic conditions by using dry argon gas and a Schlenck apparatus. Experiments with (B)Chl *a* were performed in a dark, cold room ($5\text{ }^{\circ}\text{C}$).

For each ^1H and ^{13}C NMR experiment, $\sim 1\text{--}2\text{ mg}$ (B)Chl *a* was dissolved in 2 mL of 2-propanol for the azeotropic removal of traces of water and transferred into a two-necked round-bottom flask. The solvent was evaporated and the concentrate was exposed to vacuum (0.03 mmHg) at $40\text{ }^{\circ}\text{C}$ for 2 h. Subsequently, argon gas was led in and 500 μL of anhydrous CDCl_3 was added. A NMR tube was annealed with a burner and placed in a Schlenck apparatus. After cooling to ambient temperature under high vacuum, argon gas was led in and the prepared solution was transferred into the NMR tube. The NMR tube was covered with a rubber stopper to keep the sample in a dry argon atmosphere. For the preparation of a water-free sample of $\text{Mg}(\text{II})\text{-OEP}$, the $\text{Mg}(\text{II})\text{-OEP}$ ($\sim 1\text{--}2\text{ mg}$) was weighed in a NMR tube before the annealing procedure.

NMR/IR experiments

For ^1H and ^{13}C NMR experiments, various amounts of 0.70 mM Im or 0.60 mM 1-MeIm ligand solution, ranging from 10 to

450 μL , were injected into the NMR sample tube using a micro syringe. After each injection of ligand solution, ^1H and ^{13}C NMR spectra were recorded to determine the $\Delta\delta_{\text{H}} < 0$ and $\Delta\delta_{\text{C}} < 0$ of the ligand nuclei, relative to the corresponding shifts for the ligand molecules in solution. The $\Delta\delta_{\text{H}}$ and $\Delta\delta_{\text{C}}$ of the ligand hydrogens were measured for various r_{m} values, starting at the lowest ligand concentration. The r_{m} was determined from the integrals of the resonances in the ^1H NMR spectra.

All spectra were recorded at 298 K with a Bruker DPX spectrometer operating at 9.4 T. The δ_{H} of CHCl_3 at 7.26 ppm was used for internal calibration of the ^1H shift scale, while the response of CDCl_3 at 77.0 ppm was used for the calibration in the ^{13}C NMR spectra. For ^{15}N NMR experiments, the crystalline $[\text{Mg}(\text{II})\text{-OEP}\cdot 1,3\text{-}^{15}\text{N}, 1,2\text{-}^{13}\text{C}\text{-}1\text{-MeIm}]$ and $[\text{Mg}(\text{II})\text{-OEP}\cdot 1,3\text{-}^{15}\text{N}\text{-Im}]$ complexes were dissolved in anhydrous CDCl_3 . A relaxation delay of 10 s was used after each $\pi/4$ pulse. The δ_{N} was referenced relative to the response of liquid NH_3 with $\delta_{\text{N}} = 0.0\text{ ppm}$. $^1\text{H}\text{-}^{15}\text{N}$ correlations were determined using the heteronuclear multiple bond correlation (HMBC) solution NMR technique. A ^{15}N solid-state MAS NMR spectrum from the crystalline $[\text{Mg}(\text{II})\text{-OEP}\cdot 1,3\text{-}^{15}\text{N}, 1,2\text{-}^{13}\text{C}\text{-}1\text{-MeIm}]$ complex prepared in a 4.0 mm CRAMPS rotor was recorded, using a DMX-400 Bruker NMR spectrometer. The $\Delta\delta_{\text{N}}$ values were determined from the ^{15}N shifts in solution, since the pure 1-MeIm is a liquid and cannot be measured in the solid state.

From the crystalline $[\text{Mg}(\text{II})\text{-OEP}\cdot \text{H}_2\text{O}]$ and $[\text{Mg}(\text{II})\text{-OEP}\text{-diazole}]$ complexes, IR spectra between 4000 and 300 cm^{-1} were recorded on a Perkin-Elmer Paragon 1000 FTIR spectrometer. To observe the $\text{Mg}\text{-N}_4(\text{por})$, $\text{Mg}\text{-O}_{\text{H}_2\text{O}}$ and $\text{Mg}\text{-N}_{\text{diazole}}$ vibration frequencies, far-IR spectra of the crystalline $[\text{Mg}(\text{II})\text{-OEP}\cdot \text{H}_2\text{O}]$, the $[\text{Mg}(\text{II})\text{-OEP}\cdot 1,3\text{-}^{15}\text{N}\text{-Im}]$ and the $[\text{Mg}(\text{II})\text{-OEP}\cdot 1,3\text{-}^{15}\text{N}, 1,2\text{-}^{13}\text{C}\text{-}1\text{-MeIm}]$ complexes were recorded between 150 and 400 cm^{-1} on a Bruker 113v IR spectrometer.

Results

^1H NMR spectroscopy was used to determine the molar ratio of $\text{Mg}(\text{II})\text{-Por}$ to ligand by the integrals of the ^1H responses and for an accurate determination of the ring current effect. Because it was expected that the carbon and nitrogen atoms are more changed by the electronic structure than the hydrogen atoms connected to the ligand, ^{15}N NMR and ^{13}C NMR experiments were applied to provide insight into the electronic structure of the axially coordinated ligand. In particular, ^{15}N NMR experiments were performed to deduce the electronic change of the nitrogen when it coordinates to the $\text{Mg}(\text{II})\text{-Por}$ complex. IR spectra were recorded to complement and to confirm the NMR results.

^1H NMR

To determine the $\Delta\delta_{\text{H}}$, $\Delta\delta_{\text{C}}$ and $\Delta\delta_{\text{N}}$ values, first the isotropic chemical shifts of the free Im and 1-MeIm in CDCl_3 were determined. The δ_{H_2} , δ_{H_4} and δ_{H_5} values of Im in CDCl_3 are 7.72, 7.02 and 7.02 ppm, respectively. For 1-MeIm, chemical shifts were measured for δ_{H_2} , δ_{H_4} , δ_{H_5} and δ_{CH_3} at 7.42, 6.87, 7.05 and 3.68 ppm, respectively. The δ_{C_1} and δ_{C_2} positions are observed at 137.9 and 33.3 ppm. The δ_{C_2} of free $[1,3\text{-}^{15}\text{N}, 2\text{-}^{13}\text{C}]\text{-Im}$ in CDCl_3 is 134.9 ppm. The δ_{N_1} and δ_{N_3} of free $[1,3\text{-}^{15}\text{N}, 1,2\text{-}^{13}\text{C}]\text{-}1\text{-MeIm}$ are 161.2 and 256.1 ppm,

respectively. The individual δ_{N1} and δ_{N3} of [1,3- ^{15}N ,2- ^{13}C]-Im cannot be determined, because of the tautomerization that yields $\delta_{N1,N3} = 209.1$ ppm.

To resolve the $\Delta\delta_{\text{H}}$ of the ligand atoms, Mg(II)-OEP and (B)Chl *a* were titrated with aliquots of Im or 1-MeIm solutions. As an example, NMR spectra of a titration series of 1-MeIm and BChl *a* are shown in Fig. 2. The maximum coordination shift ($\Delta\delta_{\text{H}}^{\text{max}}$), from the diamagnetic ring current effect of the porphyrin macrocycle, is observed for $r_m \leq 1.0$. The $\Delta\delta_{\text{H}}$ value decreases for $r_m > 1.0$ and vanishes for $r_m \rightarrow \infty$. The δ_{H5} and δ_{CH3} can be followed from the first added aliquot of ligand solution, since the resonances of the ligand are well resolved against the Mg(II)-OEP or (B)Chl *a* background, while the responses from δ_{H2} and δ_{H4} are broadened and cannot be resolved for $r_m < 1.0$. Both the line width and the $\Delta\delta_{\text{H}}$ are larger for H2 and H4 than for the other ligand hydrogens. For $r_m < 1.0$, the observed $\Delta\delta_{\text{H5}}$ and $\Delta\delta_{\text{CH3}}$ are at their maximum and do not change when r_m is increased. For $r_m > 1.0$, the $\Delta\delta_{\text{H5}}$ and the $\Delta\delta_{\text{CH3}}$ decrease after addition of each new aliquot of ligand. $\Delta\delta_{\text{H2}}$ and $\Delta\delta_{\text{H4}}$ appear as broad signals when $r_m > 4.3$. These signals narrow when the

r_m is increased, while the ring-current shifts also vanish for $r_m \rightarrow \infty$.

Evidently, an excess of Mg(II)-Por leads to coordination of all available Im or 1-MeIm, leading to the maximum $\Delta\delta_{\text{H}}$. All titration experiments consistently show stronger ring-current effects for H2 and H4 than for H5 and CH_3 . While for the free Im the H4 and H5 resonances have the same isotropic shift due to the fast exchange between the two tautomeric forms, a different ring-current effect on H4 and H5 due to coordination makes them distinguishable. At a r_m of approximately 7.5 the δ_{H2} and the δ_{H5} are identical (Fig. 2). In all series, the crossing point of the δ_{H2} and the δ_{H5} is found at ~ 6.5 ppm. The $\Delta\delta_{\text{H}}^{\text{max}}$ results for Im and 1-MeIm in the titration series with Mg(II)-OEP or (B)Chl *a* as a ring-current reagent are summarized in Table 1. For the [(B)Chl *a*-diazole] complexes the $\Delta\delta_{\text{H2}}^{\text{max}}$ and $\Delta\delta_{\text{H4}}^{\text{max}}$ are not observed owing to broadening of the signals or overlap with the (B)Chl *a* porphyrin background signal. In contrast, for the relatively simple [Mg(II)-OEP-diazole] complexes, a $\Delta\delta_{\text{H}}^{\text{max}}$ is observed for all ligand hydrogens.

For the titration series with Mg(II)-OEP the $\Delta\delta_{\text{H2}}^{\text{max}}$, $\Delta\delta_{\text{H4}}^{\text{max}}$, $\Delta\delta_{\text{H5}}^{\text{max}}$ and $\Delta\delta_{\text{CH3}}^{\text{max}}$ are all observed and the titration curves of the $\Delta\delta$ can be scaled by setting $\Delta\delta_{\text{H}}^{\text{max}} = 1.0$. As an example, we show in Fig. 3A the scaled titration curves of $\Delta\delta_{\text{H2}}$, $\Delta\delta_{\text{H4}}$, $\Delta\delta_{\text{H5}}$ and $\Delta\delta_{\text{CH3}}$ of the 1-MeIm for various r_m values. The four $\Delta\delta$ curves are comparable. This reflects that the variation of $\Delta\delta$ with r_m is due to the same molecular events for all hydrogens. Similar behavior is observed for the $\Delta\delta_{\text{H2}}$, $\Delta\delta_{\text{H4}}$ and $\Delta\delta_{\text{H5}}$ of the Im ligand coordinated to Mg(II)-OEP. For the (B)Chl *a* series, only $\Delta\delta_{\text{H5}}$ and $\Delta\delta_{\text{CH3}}$ curves can be compared, since the $\Delta\delta_{\text{H2}}^{\text{max}}$ and $\Delta\delta_{\text{H4}}^{\text{max}}$ are not observed for $r_m < \sim 4.0$. However, when the observable parts of the $\Delta\delta_{\text{H2}}$ and $\Delta\delta_{\text{H4}}$ curves for $r_m > \sim 4.0$ are scaled also, a good correlation with the $\Delta\delta_{\text{H5}}$ and $\Delta\delta_{\text{CH3}}$ normalized data is obtained. Subsequently, the $\Delta\delta_{\text{H2}}^{\text{max}}$ and $\Delta\delta_{\text{H4}}^{\text{max}}$ were estimated by extrapolation. For the titration series in which Im was added to (B)Chl *a*, no full $\Delta\delta_{\text{H5}}^{\text{max}}$ titration curve was observed, since $\Delta\delta_{\text{H5}}$ in the [(B)Chl *a*-Im] complexes is broadened for $r_m < 1.0$. In this case, it is not possible to scale the $\Delta\delta_{\text{H5}}^{\text{max}}$ to 1.0, which is necessary for the extrapolation of the $\Delta\delta_{\text{H2}}$ and $\Delta\delta_{\text{H4}}$ curves.

The $\Delta\delta_{\text{Hmeso}}$ (H5, H10, H15 and H20 of the Mg(II)-OEP) values show a small significant gradual increase for $r_m < 1.0$ and reach $\Delta\delta_{\text{Hmeso}}^{\text{max}}$ at $r_m = 1.0$. For $0.0 < r_m \leq 1.0$, the $\Delta\delta_{\text{H}}$ of the ligand is maximal and does not change. The increase of the $r_m > 1.0$ yields a decrease of the $\Delta\delta_{\text{H}}$ of the ligand hydrogens (Fig. 3A), while the $\Delta\delta_{\text{Hmeso}}^{\text{max}}$ is essentially constant for $r_m > 1.0$ (Fig. 3B). The ethyl groups of Mg(II)-OEP are hardly affected by the axial coordination. A $\Delta\delta_{\text{Hmeso}}^{\text{max}}$ for $\Delta\delta_{\text{H5}}$, $\Delta\delta_{\text{H10}}$ and $\Delta\delta_{\text{H20}}$ of the pure [(B)Chl *a*-diazole] complex dissolved in CDCl_3 cannot be derived, since the δ_{H5} , δ_{H10} and δ_{H20} signals are broadened beyond the detection limit owing to aggregation of the chlorophyll molecules. When a small amount of ligand is added,

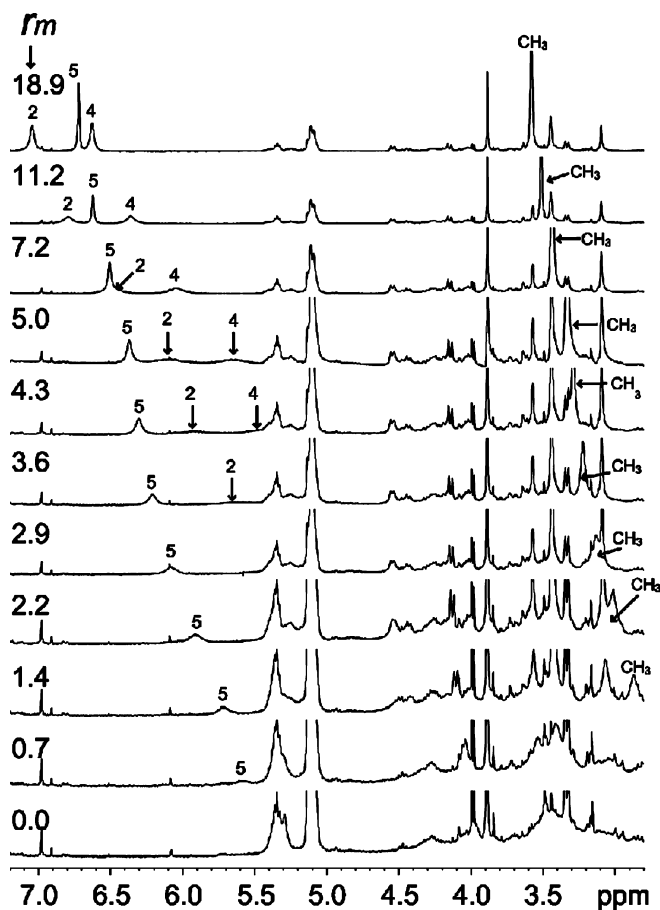


Fig. 2 ^1H coordination shifts of 1-MeIm as function of [1-MeIm]:[(B)Chl *a*] molar ratios (r_m), measured in CDCl_3 at 25°C . The signals from δ_{H2} and δ_{H4} are indicated by arrows

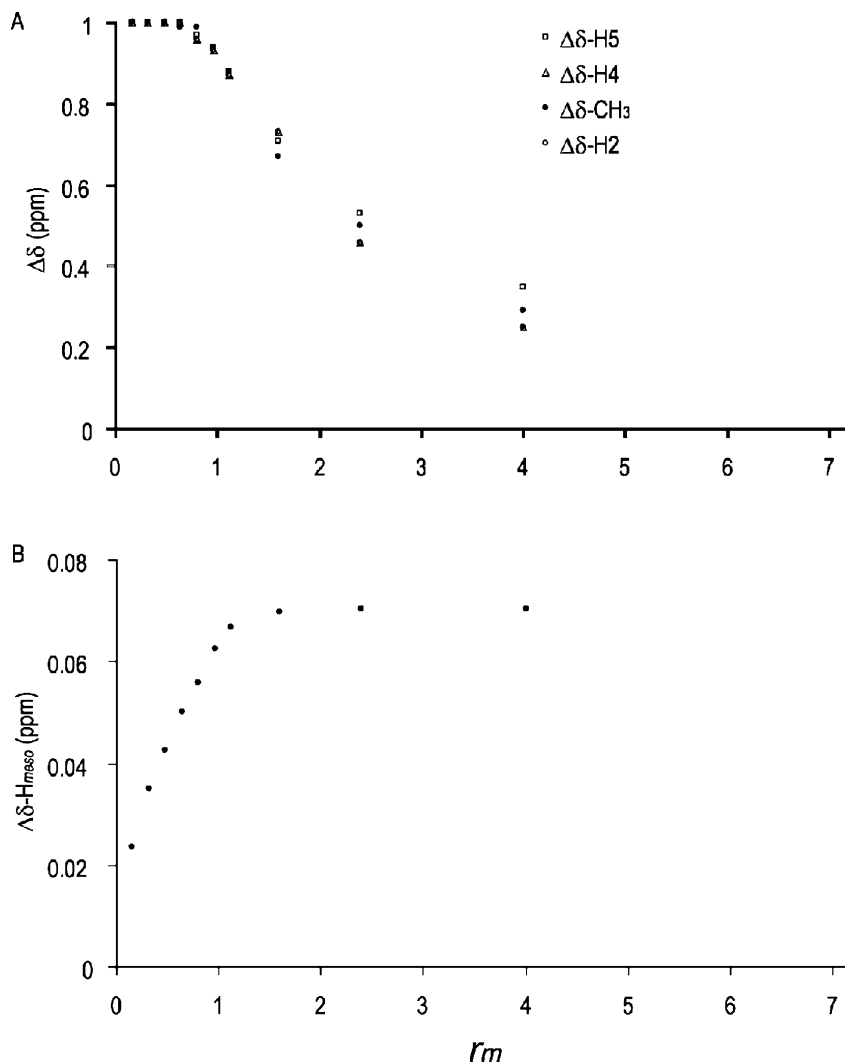
Table 1 $\Delta\delta_{\text{H}}^{\text{max}}$, $\Delta\delta_{\text{C}}^{\text{max}}$ and $\Delta\delta_{\text{N}}^{\text{max}}$ values (ppm) for imidazole and 1-methyl imidazole coordinated to Mg(II)-OEP and (B)Chl *a*

Im complex	H ₂	H ₄	H ₅	NH	H- <i>meso</i>	C ₂			
Mg(II)-OEP	4.9	4.7	2.3	4.2	0.08	4.5			
Chl <i>a</i>	–	–	1.6 ^a	–	–	–			
BChl <i>a</i>	–	–	1.0 ^a	–	–	–			
1-MeIm complex	H ₂	H ₄	H ₅	CH ₃	H- <i>meso</i>	C ₂	CH ₃	N ₁	N ₃
Mg(II)-OEP	5.2	5.2	2.3	1.6	0.07	5.5	1.3	2.1	27.2
Chl <i>a</i>	3.0 ^b	3.0 ^b	1.7	1.1	–	–	–	–	–
BChl <i>a</i>	2.8 ^b	2.7 ^b	1.5	0.9	–	2.2	0.2	–	–

^aObservable for $r_{\text{m}} > \pm 2.5$ ^bExtrapolated values

Fig. 3 A Normalized $\Delta\delta_{\text{H}}$ values of the ligand hydrogens in the [Mg(II)-OEP-1-MeIm] complex for various r_{m} values, measured in CDCl₃ at 25 °C.

B $\Delta\delta_{\text{H-*meso*}}$ of [Mg(II)-OEP-1-MeIm] for various r_{m} values, measured in CDCl₃ at 25 °C. The *dashed line* marks the $r_{\text{m}} = 1.0$ point of the equimolar ratio in the titration series



broad δ_{H5} , δ_{H10} and δ_{H20} signals are observed that are not shifted. The δ_{H5} , δ_{H10} and δ_{H20} signals narrow upon increasing r_{m} to $r_{\text{m}} = 1.0$.

¹³C and ¹⁵N NMR

The $\Delta\delta_{\text{C2}}^{\text{max}}$ and $\Delta\delta_{\text{CH3}}^{\text{max}}$ values for the [1,3-¹⁵N,2-¹³C]-Im and [1,3-¹⁵N,1,2-¹³C]-1-MeIm complexes

are summarized in Table 1. The coordination effects on the $\Delta\delta_{\text{C}}$ values, due to ring currents and electronic perturbations when Im or 1-MeIm coordinates to Mg(II), are consistent with the effects measured for $\Delta\delta_{\text{H}}$. Also a gradual decrease of $\Delta\delta_{\text{C}}$ is observed for $r_{\text{m}} > 1.0$.

For the ¹⁵N NMR measurements, the HMBC technique that provides the ¹H-¹⁵N correlations was performed on the crystalline [Mg(II)-OEP-1,3-¹⁵N,1,

2- ^{13}C -1-MeIm] and [Mg(II)-OEP·1,3- ^{15}N -Im] complexes dissolved in anhydrous CDCl_3 . The r_m is exactly 1.0, pointing to a single axial coordination of the Mg(II)-Por complex. The $\Delta\delta_{\text{H}}^{\text{max}}$ values of the ligand hydrogens can be detected in the ^1H NMR spectrum and are in line with the $\Delta\delta_{\text{H}}^{\text{max}}$ obtained from the titration series. The HMBC NMR spectrum of the [Mg(II)-OEP·1,3- ^{15}N ,1,2- ^{13}C -1-MeIm] complex is presented in Fig. 4. Strong signals are observed for the $^{15}\text{N1}/\text{CH}_3$ and the $^{15}\text{N1}/\text{H5}$ correlation, while weaker correlation signals are observed for the $^{15}\text{N1}/\text{H2}$, $^{15}\text{N3}/\text{H2}$, $^{15}\text{N3}/\text{H4}$ and the $^{15}\text{N3}/\text{H5}$ cross resonances. The 2D NMR spectrum also shows a correlation between the δ_{Hmeso} at 10.1 ppm and the natural abundance signal from the four N nuclei of Mg(II)-OEP at $\delta_{\text{N}}=200$ ppm. The $^{15}\text{N}_1$ and $^{15}\text{N}_3$ are detected with $\delta_{\text{N1}}=159.1$ and $\delta_{\text{N3}}=230.9$ ppm, corresponding to a $\Delta\delta_{\text{N}}^{\text{max}}$ of 2.1 and 25.2 ppm, respectively. This is also shown in Fig. 5D. The strong $^1J(^1\text{H}-^{13}\text{C})$ couplings between H2 and $^{13}\text{C2}$ (206 Hz) and between $^{13}\text{CH}_3$ and $^{13}\text{CH}_3$ (140 Hz) confirm the assignment of both nitrogen signals. When the r_m is increased to 2.5, the δ_{N3} broadens beyond the detection limit. This indicates exchange of the coordinated 1-MeIm with the 1-MeIm pool in solution. For $r_m > 10$ the ^{15}N NMR spectrum is essentially identical to the spectrum observed for the free ligand solution.

The HMBC NMR spectrum of the [Mg(II)-OEP·1,3- ^{15}N -Im] complex (data not shown) clearly shows the $^{15}\text{N1}/\text{NH1}$ ($^1J(^1\text{H}-^{15}\text{N})=96$ Hz) and the $^{15}\text{N1}/\text{H5}$ correlation. The correlation between the δ_{Hmeso} at 10.1 ppm and the natural abundance δ_{N} of the

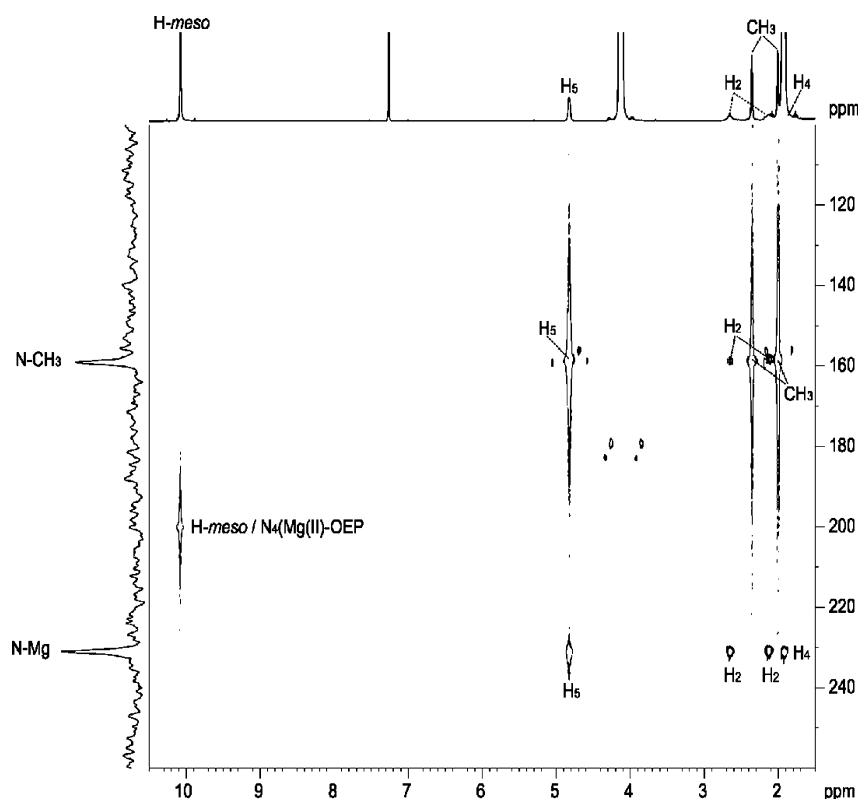
Mg(II)-OEP at 200 ppm is also observed. The correlations $^{15}\text{N3}/\text{H2}$, $^{15}\text{N3}/\text{H4}$ and $^{15}\text{N3}/\text{H5}$ are too weak to be detected. The 1D solution ^{15}N NMR spectrum of the [Mg(II)-OEP·1,3- ^{15}N -Im] complex in Fig. 5B shows two ^{15}N signals at 232.9 and 154.0 ppm from N3-Mg and N1H ($^1J(^1\text{H}-^{15}\text{N})=96$ Hz), respectively. These isotropic chemical shifts are comparable to the ^{15}N shifts measured for the [Mg(II)-OEP·1,3- ^{15}N ,1,2- ^{13}C -1-MeIm] complex. The averaged δ_{N1} and δ_{N3} of free [1,3- ^{15}N]-Im in solution makes it impossible to determine $\Delta\delta_{\text{N}}$ in solution.

Figure 5E shows the 1D MAS NMR spectrum of the [Mg(II)-OEP·1,3- ^{15}N ,1,2- ^{13}C -1-MeIm] complex. The measurement demonstrates the existence of the model complex in the solid state, and that it has exactly one axial ligand, forming a five-coordinated complex, which corresponds with the (B)Chl *a*-his(Im) complex natural photosynthetic complexes [4]. The $\Delta\delta_{\text{N}}$ provided by the MAS ^{15}N NMR spectra of the [Mg(II)-OEP·1,3- ^{15}N ,1,2- ^{13}C -1-MeIm] complex are in close agreement with the shifts observed for the monomeric complex in solution. The δ_{N3} (N3-Mg) appears at 229 ppm and corresponds with $\Delta\delta_{\text{N}}=27.2$ ppm. The $\Delta\delta_{\text{N1}}$ shift is only 0.8 ppm.

IR spectra

To complement the NMR data, we have recorded a few IR data sets from the complexes. The O–H stretching vibration in the IR spectrum of [Mg(II)-OEP·H₂O] at

Fig. 4 ^1H - ^{15}N HMBC NMR correlation dataset of microcrystalline [Mg(II)-OEP·[1,3- ^{15}N ,1,2- ^{13}C]-1-MeIm] dissolved in CDCl_3 . The large $\Delta\delta_{\text{H2}}^{\text{max}}$, $\Delta\delta_{\text{H4}}^{\text{max}}$ and $\Delta\delta_{\text{H5}}^{\text{max}}$ and the relative signal intensity in the ^1H NMR, in combination with the correlation between H₂, H₄, H₅ and the 1- ^{15}N at 231 ppm, prove the existence of the five-coordinated [Mg(II)-OEP $^{\delta-}$ /1-MeIm $^{\delta+}$] complex



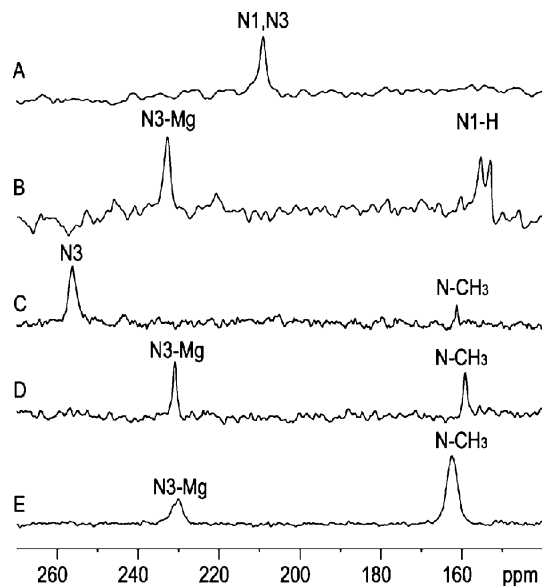
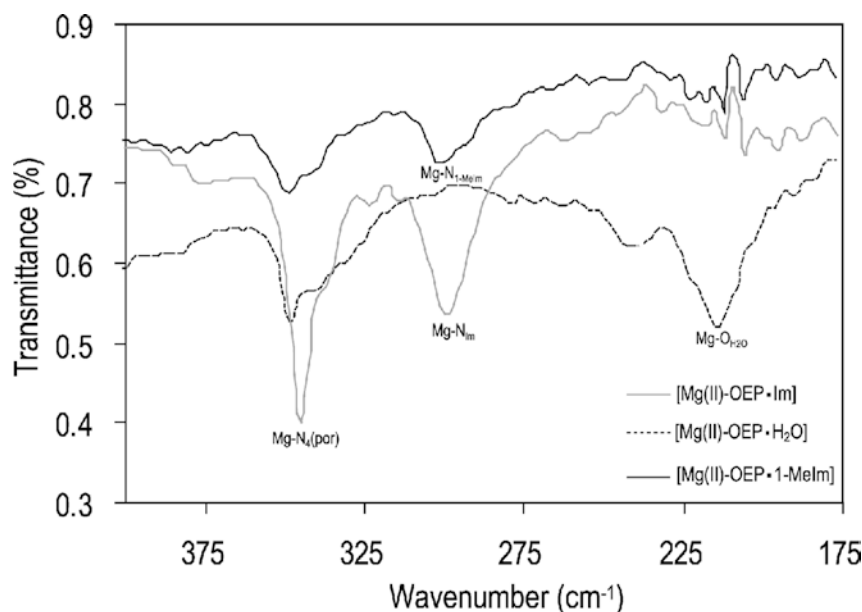


Fig. 5 ^{15}N NMR spectra of free $[1,3-^{15}\text{N}]\text{-Im}$ (A), the monomeric $[\text{Mg}(\text{II})\text{-OEP}\cdot 1,3-^{15}\text{N}\text{-Im}]$ complex $[^1J(\text{H}-^{15}\text{N}) = 96 \text{ Hz}]$ (B), free $[1,3-^{15}\text{N}, 1,2-^{13}\text{C}]\text{-1-MeIm}$ (C), the monomeric $[\text{Mg}(\text{II})\text{-OEP}\cdot 1,3-^{15}\text{N}, 1,2-^{13}\text{C}\text{-1-MeIm}]$ complex in CDCl_3 (D), and a MAS NMR spectrum of the crystalline $[\text{Mg}(\text{II})\text{-OEP}\cdot 1,3-^{15}\text{N}, 1,2-^{13}\text{C}\text{-1-MeIm}]$ complex (E)

3529 cm^{-1} (data not shown) has disappeared in the spectra of the $[\text{Mg}(\text{II})\text{-OEP}\cdot 1,3-^{15}\text{N}\text{-Im}]$ and $[\text{Mg}(\text{II})\text{-OEP}\cdot 1,3-^{15}\text{N}, 1,2-^{13}\text{C}\text{-1-MeIm}]$ complexes. This shows that a water molecule is substituted by Im and 1-MeIm, respectively. In the IR spectrum of the $[\text{Mg}(\text{II})\text{-OEP}\cdot 1,3-^{15}\text{N}\text{-Im}]$ complex, a response is observed at 3347 cm^{-1} , which is assigned to the N–H stretching vibration of the axially coordinated Im.

The low-frequency region in the far-IR spectra of all three complexes is presented in Fig. 6. It shows a vibration at 350 cm^{-1} with a shoulder at $\sim 340 \text{ cm}^{-1}$.

Fig. 6 Low-frequency IR spectra of the $[\text{Mg}(\text{II})\text{-OEP}\cdot \text{H}_2\text{O}]$ complex (dashed line), the crystalline $[\text{Mg}(\text{II})\text{-OEP}\cdot 1,3-^{15}\text{N}, 1,2-^{13}\text{C}\text{-1-MeIm}]$ complex (solid line) and the $[\text{Mg}(\text{II})\text{-OEP}\cdot 1,3-^{15}\text{N}\text{-Im}]$ complex (grey line)



These vibrations are assigned to the symmetric and asymmetric $\text{Mg}\text{-N}_4(\text{Por})$ stretching vibrations, respectively. Upon substitution of the axial water ligand by Im or 1-MeIm, the $\text{Mg}\text{-O}_{\text{H}_2\text{O}}$ stretching vibration at 215 cm^{-1} disappears and a new response from the $\text{Mg}\text{-N}_{1\text{-MeIm}}$ or $\text{Mg}\text{-N}_{\text{Im}}$ stretching vibration can be observed at 300 cm^{-1} , pointing to a dynamic complex.

Discussion

Monomeric (B)Chl, dissolved in polar solvents, shows very sharp and narrow resonances in the ^1H NMR spectra [16]. (B)Chl *a* in CDCl_3 is aggregated, and does not form solvate complexes [20, 21]. In our model study this is reflected by the broadened signals for the H_5 , H_{10} and H_{20} *meso*-hydrogens ($\delta_{\text{H}_{\text{meso}}}$) from pure (B)Chl *a* in CDCl_3 . The δ_{H_5} , $\delta_{\text{H}_{10}}$ and $\delta_{\text{H}_{20}}$ responses of (B)Chl *a* show up gradually and narrow when Im or 1-MeIm is added to the (B)Chl *a* solution. This shows that axial ligand coordination is energetically favorable compared to maintaining an aggregate structure. For $r_m \geq 1.0$, the H_{meso} resonances are narrow, and do not show an up-field shift due to neighboring porphyrins like occurs in aggregate structures. This provides evidence for the formation of the $[(\text{B})\text{Chl } \alpha\text{-diazole}]$ complex in CDCl_3 . The $\delta_{\text{H}_{\text{meso}}}$ of the $[\text{Mg}(\text{II})\text{-OEP}\cdot \text{H}_2\text{O}]$ and the $\delta_{\text{H}_{\text{meso}}}$ of the $[\text{Mg}(\text{II})\text{-OEP}\cdot \text{diazole}]$ complexes are narrow for both $r_m < 1.0$ and $r_m \geq 1.0$ and are not shifted due to the aggregation effects, which gives convincing evidence for monomeric $[\text{Mg}(\text{II})\text{-OEP}\cdot \text{H}_2\text{O}]$ and $[\text{Mg}(\text{II})\text{-OEP}\cdot \text{diazole}]$ complexes in CDCl_3 .

A constant $\Delta\delta_{\text{H}}$ in all titration experiments at $r_m < 1.0$ shows that virtually all added ligand molecules are coordinated to the $\text{Mg}(\text{II})$ ion. The decrease of the $\Delta\delta_{\text{H}}$ for $r_m > 1.0$ is attributed to a rapid exchange of coordinated ligand with molecules from the ligand pool, since in that

case averaging of the isotropic shifts of the coordinated and free ligand occurs, according to their relative concentrations (Fig. 2).

The $\delta_{\text{H}_{\text{meso}}}$ for $r_m < 1.0$ is due to rapid averaging of the responses from the coordinated and bare porphyrin. In that case, all the available ligand is coordinated and the excess of Mg(II)-Por exchanges with the coordinated form. At $r_m = 1.0$ the $\Delta\delta_{\text{H}_{\text{meso}}}^{\text{max}}$ is reached, while at this point the decrease of the $\Delta\delta_{\text{H}}$ of the ligand starts. This means a minimum of exchange at $r_m = 1.0$.

Since the $\Delta\delta_{\text{H}_{\text{meso}}}^{\text{max}}$ is reached for $r_m \geq 1.0$ (Fig. 3B), it can be concluded that the Mg(II)-Por complexes in solution are five-coordinated. The binding of N-donor ligands in solution to Mg(II)-Por, like pyridines and diazoles, has been studied thoroughly and it is clear that the dominant process in solution and in most crystal structures is the formation of five-coordinate 1:1 adducts that have a puckered structure [17, 18, 19]. Axial coordination to the Mg(II) of (B)Chl *a* has been investigated for monomeric BChl *a* complexes in solution by resonance Raman spectroscopy, magnetic circular dichroism and absorption spectroscopy [20, 21, 22, 23]. These studies confirm that the Mg(II) in (B)Chl is mostly five-coordinated in aggregates and in solution with imidazole derivatives.

The $\Delta\delta_{\text{H}}^{\text{max}}$ of the [Mg(II)-OEP-1-MeIm] and [Mg(II)-OEP-Im] complexes, summarized in Table 1, show that $\Delta\delta_{\text{H}}^{\text{max}}$ for all ligand hydrogens is slightly larger for 1-MeIm than for Im, which is in line with a stronger coordination effect for the 1-MeIm than for Im. In line with the $\Delta\delta_{\text{H}}$ results, the larger $\Delta\delta_{\text{C}2}$ for the [Mg(II)-OEP-1-MeIm] complex than for the [Mg(II)-Por-Im] complex confirms the stronger coordination effect for 1-MeIm than for Im. This stronger coordination is a result of the methyl group, which is a better electron-donating group than a hydrogen atom.

The C2 in the diazole ring is probably more sensitive to variations of the electronic structure due to coordination than the hydrogens that are connected to the ring. However, the $\Delta\delta_{\text{C}2}$ and $\Delta\delta_{\text{CH}_3}$ both decrease when $r_m > 1.0$, very similar to the $\Delta\delta_{\text{H}}$ in the titration series. This shows that $\Delta\delta_{\text{C}}$ is to a large extent determined by the ring current. The $\Delta\delta_{\text{C}2}^{\text{max}}$ in our experiments is 4.5 and 5.3 ppm for coordinated Im and 1-MeIm to Mg(II)-OEP, respectively, while the $\Delta\delta_{\text{C}2}$ of Im and 1-MeIm coordinated to BChl *a* are 1.8 and 2.2 ppm, respectively. The data for the C2 in the [Mg(II)-OEP-diazole] models match very well, with $\Delta\delta_{\text{C}} = 5.1$ ppm for the corresponding C ϵ of the histidyl residue in the natural LH2 complex [24]. This shows that the Mg-N3 coordination in the natural system is stronger than in the [BChl *a*-1-MeIm] model complex. In this regard, the stabilizing effect on the coordination bond of the methyl group at the N $^{\pi}$ in our model system provokes a comparable effect for the protein environment on the stabilization of the Mg-N coordination bond in the natural system. The protein potentially has an electron donating effect on the NH1 moiety.

The intermolecular nuclear shielding is a probe for the distance from the nucleus to the plane of the

macrocycle [25]. The ring-current effects depend more strongly on the distance to the plane of the macrocycle for nuclei at a short distance than for positions that are more remote from the equatorial plane [25, 26, 27]. Therefore, the $\Delta\delta$ for nuclei closer to the porphyrin ring are more sensitive to variations in the distance than the $\Delta\delta$ of nuclei that are remote. Owing to vibrations of the Mg-N bond as found by the IR measurements, the distance between the nuclei and the macrocycle slightly changes continuously, yielding a broadened response of the ligand nuclei. This is reflected in the line widths, which are larger for the proximal H2 and H4 than for the distal H5 and the CH₃. From the equal $\Delta\delta_{\text{H}2}^{\text{max}}$ and $\Delta\delta_{\text{H}4}^{\text{max}}$ (Table 1), it is concluded that the distances between H2 and the macrocycle and between H4 and the macrocycle are equal. As a consequence of the symmetry of the ligand, the distances between H5 and the macrocycle and between NH1 and the macrocycle are also equal. It is remarkable that the H1 in the [Mg(II)-OEP-Im], with $\Delta\delta_{\text{NH}1}^{\text{max}} = 4.2$ ppm, is more shielded than the H5, with $\Delta\delta_{\text{H}5}^{\text{max}} = 2.3$ ppm, while the distances for H5 and NH1 to the Mg(II) should be comparable, according to electronic calculations performed on this model system, which show that an identical shielding effect can be expected for both H5 and NH1 (unpublished results). Moreover, the $\Delta\delta_{\text{NH}1}$ titration curve cannot be scaled to the normalized curves for $\Delta\delta_{\text{H}2}$, $\Delta\delta_{\text{H}4}$ and $\Delta\delta_{\text{H}5}$. This indicates that $\Delta\delta_{\text{NH}1}$ cannot be only a result of the ring-current effect and involves another mechanism as well. The NH1 signal of free Im in solution is observed at 10.8 ppm, which is significantly higher than the calculated value of 8.1 ppm, while all other calculated shifts correspond with the observed values in the blank experiment. We attribute the relatively high $\delta_{\text{NH}1}$ of Im in solution to intermolecular hydrogen-nitrogen interactions of Im molecules, forming loose aggregates, while the calculations are performed on a monomer. For the [Mg(II)-OEP-Im] complex, the calculated $\delta_{\text{NH}1} = 6.1$ and the observed $\delta_{\text{NH}1} = 6.6$ are comparable, which confirms that $\delta_{\text{NH}1}$ of Im in solution is anomalous.

The HMBC NMR spectrum of the dissolved crystalline [Mg(II)-OEP-1,3-¹⁵N,1,2-¹³C-1-MeIm] complex, presented in Fig. 4, shows that the exchange processes are quenched exactly at the equimolar ratio when $r_m = 1.0$ and a stable complex is obtained in solution. This is in line with the ¹H NMR spectra. Both the pyrrole- and the pyridine-type ¹⁵N are observed, while the pyridine-type ¹⁵N cannot be observed in the ¹⁵N NMR data sets of the titration series owing to exchange broadening. The $\delta_{\text{N}3}$ (N-Mg) at 230.9 ppm in the HMBC NMR spectrum of the [Mg(II)-OEP-1,3-¹⁵N,1,2-¹³C-1-MeIm] complex in CDCl₃ and at 228.9 ppm in the ¹⁵N MAS NMR data set implies a $\Delta\delta_{\text{N}}$ of 25.2–27.2 ppm. Such a large $\Delta\delta_{\text{N}}$ cannot be produced by ring currents, and provides convincing evidence for a strongly perturbed electronic structure. The shift of the $\delta_{\text{N}3}$ (N-Mg) is close to the $\delta = 224.0$ ppm observed for the $\delta_{\text{N}3}$ (N-Mg) in the LH2 antenna complex [6]. The

large $\Delta\delta_{\text{N}}^{\text{max}}$ of the N3 (N–Mg) possibly points to a partial charge transfer from the 1-MeIm to the Mg(II)-OEP, yielding a Mg(II)-OEP^{δ-}/1-MeIm^{δ+} complex, which was observed for the natural LH2 complex [24]. In a more general perspective, the coordination of histidine and imidazole in the model compounds are also of interest for studies of other porphyrin- or heme-containing proteins that have dynamic axial coordination properties to perform their biological key function.

The $\Delta\delta$ is a useful marker to provide insight into the axial coordination of diazole ligands coordinated to Mg(II) porphyrins. The $\Delta\delta_{\text{H}}$ data compare well with previous results from other Mg(II)-porphyrin systems that also show a gradual change of the $\Delta\delta_{\text{H}}$ after increasing the methanol or pyridine concentrations [28, 29]. In all cases, the NMR measurements were done in a non-polar solvent.

Finally, in the NMR study on the [(B)Chl *a*-Im] complex in THF, relatively small shifts (<0.5 ppm) were found for the coordinated Im hydrogens and no coordination was observed when 1-MeIm was co-dissolved with (B)Chl *a* in THF [8]. In this study, a negatively charged [(B)Chl *a*-Im] complex was inferred to explain the results. In the present study, we observe a single neutral axial coordination for both the [Mg(II)-Por-1-MeIm] and [Mg(II)-Por-Im] complexes in CDCl₃, with large hydrogen shifts for both coordinated Im and 1-MeIm.

Acknowledgements We thank F. Lefeber and J. Hollander for their help with the NMR measurements, G. van Albada for help with the IR measurements, S. Touw for valuable discussions about the interpretation of the coordination shifts with the help of molecular calculations, E. Schulten for giving additional information for the isolation of the (B)Chls, and P. Gast for using the laboratory facilities to grow the bacteria. This research was supported in part by demonstration Project B104-CT97-2101 of the commission of the European Communities. H.J.M.dG. is a recipient of the PIONEER award of the chemical sciences section of the Netherlands Organization for scientific research (NWO).

References

- Scheer H (ed) (1991) Chlorophylls. CRC Press, Boca Raton, Fla., USA
- Branden C, Tooze J (1991) Introduction to protein structure. Garland, New York, pp 234–250
- Robert B, Lutz M (1987) Biochim Biophys Acta 807:10–23
- Prince SM, Papiz MZ, Freer AA, McDermott G, Hawthornthwaite-Lawless AM, Cogdell RJ, Isaacs NW (1997) J Mol Biol 268:412–423
- Storm CB (1970) J Am Chem Soc 92:1423–1425
- Soede-Huijbrechts C, Cappon JJ, Boender GJ, Gast P, Hoff AJ, Lugtenburg J, de Groot HJM (1998) Photosynthesis: mechanisms and effects. Kluwer, Dordrecht, p 759
- Sham YY, Muegge I, Warschel A (1998) Biophys J 74:1744–1753
- Alia, Matysik J, Erkelens C, Hulsbergen FB, Gast P, Lugtenburg J, de Groot HJM (2000) Chem Phys Lett 330:325–330
- Gridnev AA, Mihaltseva IM (1994) Synth Comm 24:1547–1555
- Witanowski M, Webb GA (1973) Nitrogen NMR. Plenum, London, p 205
- Chen BB, von Philipsborn W (1983) Helv Chim Acta 66:1537–1555
- Welleman JA, Hulsbergen FB, Verbiest J, Reedijk J (1978) J Inorg Nucl Chem 40:143–147
- Lindsey JS, Woodford JN (1995) Inorg Chem 34:1063–1069
- Omata T, Murata N (1979) Photochem Photobiol 31:183–185
- Egorova-Zachernyuk TA, van Rossum B, Boender G, Franken E, Ashurst J, Raap J, Gast P, Hoff AJ, Oschkinat H, de Groot HJM (1997) Biochemistry 36:7513–7519
- Katz JJ, Strain HH, Leussing DL, Dougherty RC (1968) J Am Chem Soc 90:784–791
- Scheidt WR, Eigenbort CW, Ogiso M, Hatano H (1987) Bull Chem Soc Jpn 60:3529
- DiMugno SG, Lin VSY, Therien MJ (1993) J Am Chem Soc 115:2513
- Taylor PN, Wylie AP, Huuskonen J, Anderson HL (1998) Angew Chem, Int Ed 37:986
- Nozawa T, Ohtomo K, Suzuki M, Morishita Y, Madigan MT (1993) Bull Chem Soc Jpn 66:231–237
- Umetsu M, Wang Z, Kobayashi M, Nozawa T (1999) Biochim Biophys Acta 1410:19–31
- Umetsu M, Wang Z, Yoza K, Kobayashi M, Nozawa T (2000) Biochim Biophys Acta 1457:106–117
- Fujiwara M, Tasumi M (1986) J Phys Chem 90:250–255
- Alia, Matysik J, Soede-Huijbrechts C, Baldus M, Raap J, Lugtenburg J, Gast P, van Gorkom H J, Hoff A J, de Groot H J M (2001) J Am Chem Soc 123:4803–4809
- Giessner-Prettre C. and Pullman B (1971) J Theor Biol 31:287–294
- Abraham RJ, Bedford GR, McNeillie D, Wright B (1980) Org Magn Reson 14:418–424
- Gouedard M, Gaudemer F, Gaudemer A, Riche C (1978) J Chem Res (S):30–31
- Brereton RG, Sanders JKM (1983) J Chem Soc Perkin Trans I:423–437
- Katz JJ, Strain HH, Leussing DL, Dougherty RC (1968) J Am Chem Soc 90:784–791